

AN IMPROVED METHOD FOR CALCULATING TROPOSPHERIC TEMPERATURE AND MOISTURE FROM SATELLITE RADIOMETER MEASUREMENTS

WILLIAM L. SMITH

National Environmental Satellite Center, ESSA, Washington, D.C.

ABSTRACT

An improved method for calculating tropospheric temperature and moisture from satellite radiometer measurements is developed. The troposphere is modeled by two temperature lapse rates and a single moisture lapse rate. These lapse rates as well as an optimum pressure level for dividing the two layers of constant lapse rate and surface temperature are calculated from three observations in the 15μ CO_2 band, an observation in the rotational water vapor band, and an observation in the 11μ window region.

Radiances observed by a balloon-borne interferometer were used to approximate filtered radiometer measurements. Solutions for tropospheric temperature and moisture from the approximated radiometer observations are shown to agree favorably with radiosonde observations for both clear and partly cloudy conditions. The computations required are only 10 percent of those required by a previously developed method.

1. INTRODUCTION

In a recent paper, the author (Smith [9]) demonstrated the feasibility of utilizing relatively broad spectral satellite radiometer measurements to calculate the major characteristics of the temperature and moisture distribution of the troposphere. The troposphere was assumed to be adequately represented by two temperature lapse rates and a single moisture lapse rate. The method utilized was basically a predictor-corrector method which involved the iterative comparison of observed and calculated mean spectral radiances. Five variables were iterated in a predetermined sequence until all the radiance residuals were reduced to sufficiently small values.

After the successful completion of this study, the National Environmental Satellite Center proposed that the five-channel Medium Resolution Infrared Radiometer (MRIR), which has successfully flown on the Nimbus meteorological satellite, be modified to provide the measurements needed to calculate the tropospheric temperature and moisture structure. Although it was planned to utilize the sequential iterative procedure initially proposed by the author, with the observations to be provided by the modified MRIR, this procedure was subsequently found to be too time consuming when applied to these types of measurements. This is primarily because this procedure requires about 200 calculations of the infrared radiance corresponding to the measured radiances. Since each measured radiance is actually an average radiance over a given spectral region which is weighted spectrally by a frequency dependent filter and detector response function, each iterative step requires a time consuming numerical integration of transmissivity in narrow frequency intervals in order to account adequately for the radiometer's response over the spectral interval of the observation.

In this paper the initially proposed predictor-corrector method is modified by approximating the solution analytically. The modification permits simultaneous iterations to be used, thereby reducing the number of calculations required. The effects of random instrumental errors are minimized by smoothing the two-lapse rate solution with respect to a single lapse rate least squares solution. The optimum pressure level for dividing the two layers of constant lapse rates is determined. Furthermore, an improved method is developed for reducing the radiance data to enable the calculation of temperature and moisture profiles in partly cloudy regions. Recent measurements taken by a NASA interferometer on a high level balloon are used to approximate the filtered radiances which would have been observed by the modified five-channel MRIR. These radiances are utilized to conduct a preliminary test of this method for both clear and partly cloudy atmospheres.

2. TROPOSPHERIC TEMPERATURE PROFILE EXPERIMENT

As indicated above, the National Environmental Satellite Center is currently directing a Tropospheric Temperature Profile Experiment. The experiment, which will consist of a modified version of the MRIR, is currently scheduled to be conducted from a manned Applications Apollo Satellite in the latter part of 1969. The radiometer will measure the radiation emitted by the earth's surface and atmosphere in the following five spectral intervals: 1) $825\text{--}975\text{ cm}^{-1}$, 2) $740\text{--}780\text{ cm}^{-1}$, 3) $730\text{--}770\text{ cm}^{-1}$, 4) $717.5\text{--}757.5\text{ cm}^{-1}$, and 5) $500\text{--}570\text{ cm}^{-1}$. The first spectral region, which is situated in the atmospheric window region of the spectrum, was chosen to provide a measurement of the earth's surface temperature and a cloud amount param-

eter necessary to obtain tropospheric structure in cloudy regions. The second, third, and fourth spectral intervals, which are situated on the short wavelength side of the 15μ CO_2 band, were chosen to provide a measure of temperature profile of the troposphere. The fifth spectral region, which is situated in the rotational water vapor absorption band, was chosen to enable the total water vapor content of the troposphere to be estimated. The average tropospheric moisture profile, which may be inferred from the total water vapor, is necessary to obtain an adequate measure of the temperature profile due to the dependence of the transmittances of the first four spectral intervals on the water vapor content of the lower troposphere.

The modified five-channel radiometer is designed to scan perpendicular to the suborbital track between nadir limits. This design enables 10 resolution elements to be obtained during each swath. Each resolution element will comprise a ground projected area of about 10 n.mi.² Ten contiguous swaths of data which will enclose a ground projected 100 n.mi.² area will provide 100 sets of radiant observations from which the average temperature and moisture profiles for the 100 n.mi.² area may be calculated by the methods outlined in this paper.

3. GENERAL CONSIDERATIONS

The average radiance measured by a satellite-borne filtered radiometer in a small spectral interval, $\Delta\nu_i$, may be related to the vertical temperature and absorbing gas profiles of a cloudless atmosphere through the integral form of the radiative transfer equation

$$I(\Delta\nu_i) = B_i(p_0)\tau_i^*(p_0) - \int_0^{p_0} B_i(p) \frac{\partial \tau_i^*(p)}{\partial p} dp \quad (1)$$

where $B_i(p) = B[\Delta\nu_i, T(p)]$ is the Planck radiance at the mean frequency of the spectral interval and temperature, $T(p)$, p is atmospheric pressure, and p_0 is the pressure at the earth's surface. The effective transmittance, $\tau_i^*(p)$, of the atmosphere is defined by

$$\tau_i^*(p) = \int_{\Delta\nu_i} \phi_i(\nu) \tau(\nu, p) d\nu / \int_{\Delta\nu_i} \phi_i(\nu) d\nu \quad (2)$$

where $\phi_i(\nu)$ is the radiometer's response function and $\tau(\nu, p)$ is the transmittance of the atmospheric gas, between the satellite and the pressure p , which is optically active at the frequency ν . Figure 1 shows the transmissivity function, $\tau_i^*(p)$, calculated for the five spectral regions of the modified MRIR from two extremely different temperature and moisture soundings. (All transmissivity calculations in this paper are made utilizing the CO_2 transmissivities given by Stull, Wyatt, and Plass [10] and the water vapor absorption coefficients tabulated by Möller and Raschke [6]. All integrations over frequency are performed in increments of 2.5 cm^{-1}) It was assumed for these calculations that the instrument

response function for each spectral interval is given by

$$\phi_i(\nu) = \cos^2 [\pi(\nu - \bar{\nu}_i)/\Delta\nu_i] \quad (3)$$

where $\bar{\nu}_i$ is the central frequency of the spectral interval. The solid curves in figure 1 pertain to a moist tropical air mass and the dashed curves pertain to a dry polar air mass. The discrepancies between these two sets of curves are primarily due to the differences in water vapor and secondarily due to the differences in the temperature distributions of the two air masses. It is apparent from (1) that the region of the troposphere upon which the total upward radiance in each spectral interval is most dependent is that region where the slope of the transmittance function is the greatest. Hence, as illustrated by figure 1, the $825\text{--}975\text{-cm}^{-1}$ radiance is most highly sensitive to variations of tropospheric structure very near the surface while the $740\text{--}780\text{-cm}^{-1}$, $730\text{--}770\text{-cm}^{-1}$, $717.5\text{--}757.5\text{-cm}^{-1}$, and $500\text{--}570\text{-cm}^{-1}$ radiances are most highly sensitive to variations in the $750\text{--}1000\text{-mb.}$, $600\text{--}850\text{-mb.}$, $300\text{--}700\text{-mb.}$, and $400\text{--}1000\text{-mb.}$ tropospheric layers, respectively. It is primarily these characteristics which led to the choice of these five spectral intervals for the calculation of tropospheric temperature and moisture profiles.

4. METHOD OF CALCULATION

Since the general method to be utilized is an iterative one, the equations are developed in a form such that the solution for the k th step is given in terms of the solution obtained for the $(k-1)$ th step. The last section of this chapter describes a convergent iterative procedure which employs these equations.

TEMPERATURE MODEL

Integrating (1) by parts and utilizing the identity

$$B_i(p_i) = B_i(p_0) - \int_{p_i}^{p_0} \frac{\partial B_i(p)}{\partial p} dp$$

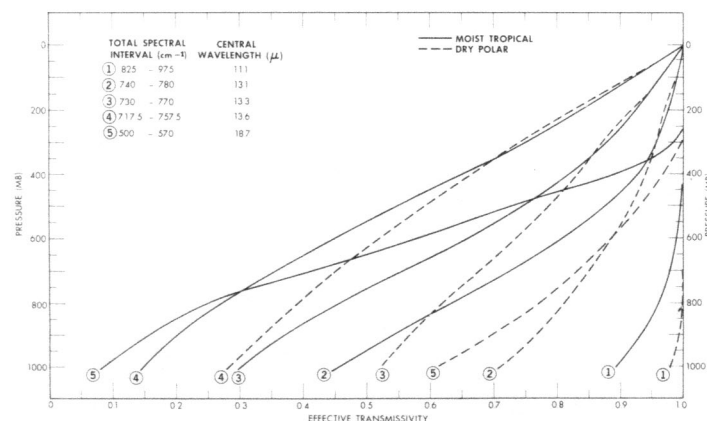


FIGURE 1.—Effective transmission between a given pressure level and the top of the atmosphere for the spectral channels and approximate filter characteristics of the Apollo MRIR. The solid and dashed curves pertain to a moist tropical and dry polar air mass, respectively.

where p_t is the tropopause pressure, one obtains the system of equations,

$$I(\Delta\nu_i) + \int_0^{p_t} B_i(p) \frac{\partial \tau_i^*(p)}{\partial p} dp = B_i(p_0) \tau_i^*(p_t) + \int_{p_t}^{p_0} [\tau_i^*(p) - \tau_i^*(p_t)] \frac{\partial B_i(p)}{\partial p} dp, \quad i=1, 2, \dots, 5. \quad (4)$$

The integral on the left in (4) represents the stratospheric contribution to the observed radiances and can be approximated sufficiently for the spectral regions considered here from the temperature distribution of a standard atmosphere. Assuming that the tropospheric temperature distribution can be adequately described by two lapse rates (as was done in a previous paper), $\partial T/\partial z$, is almost equivalent to stating that

$$T(p) = C_1 + C_2 \ln \frac{p}{p_0}, \quad p_c \leq p \leq p_0 \quad (5)$$

and

$$T(p) = C_1 + C_2 \ln \frac{p_c}{p_0} + C_3 \ln \frac{p}{p_c}, \quad p_t \leq p \leq p_c \quad (6)$$

where p_c is the pressure level dividing the layers of constant lapse rates and C_1 , C_2 , and C_3 are constants. It is apparent from (5) that $C_1 = T(p_0)$. Utilizing the approximations

$$B_i^{(k)}(p_0) = B_i^{(k-1)}(p_0) + \left[\frac{\partial B_i(p_0)}{\partial T(p_0)} \right]^{(k-1)} [T^{(k)}(p_0) - T^{(k-1)}(p_0)]$$

and

$$\frac{\partial B_i^{(k)}(p)}{\partial p} = \left[\frac{\partial B_i(p)}{\partial T(p)} \right]^{(k-1)} \frac{\partial T^{(k)}(p)}{\partial p},$$

where the superscript k refers to the k th iteration, with equations (5) and (6) and substituting into (4), one obtains

$$g_i^{(k-1)} = \sum_{j=1}^3 C_j^{(k)} a_{ij}^{(k-1)} \quad (7)$$

with

$$g_i^{(k-1)} = I(\Delta\nu_i) + \left\{ \int_0^{p_t} B_i(p) \frac{\partial \tau_i^*(p)}{\partial p} dp + \left[\frac{\partial B_i(p_0)}{\partial T(p_0)} \right]^{(k-1)} T^{(k-1)}(p_0) \tau_i^*(p_t) - B_i^{(k-1)}(p_0) \tau_i^*(p_t) \right\},$$

$$a_{i1}^{(k-1)} = \left[\frac{\partial B_i(p_0)}{\partial T(p_0)} \right]^{k-1} \tau_i^*(p_t), \quad a_{i2}^{(k-1)} = \int_{p_c}^{p_0} \alpha_i^{(k-1)}(p) dp$$

and

$$a_{i3}^{(k-1)} = \int_{p_t}^{p_c} \alpha_i^{(k-1)}(p) dp$$

where

$$\alpha_i^{(k-1)}(p) = \frac{1}{p} [\tau_i^*(p) - \tau_i^*(p_t)] \left[\frac{\partial B_i(p)}{\partial T(p)} \right]^{(k-1)}.$$

The problem of calculating the actual temperature profile from an initial estimate and the four radiance observations $I(\Delta\nu_i)$ ($i=1, \dots, 4$) reduces to that of solving the system of equations (7) for the three C 's for $k=1$. The C 's obtained

may then be used to update g_i and a_{ij} which may be used to calculate the second estimate of the temperature profile. The procedure is repeated until satisfactory convergence is reached. However, the errors in the radiance measurements may cause the iterative process to diverge if the matrix of a_{ij} is ill conditioned with respect to inversion.

A minimization procedure for overcoming the effects of random observational errors on the solution is outlined by Phillips [7] and Twomey [11]. In these papers, the error which always exists in a measured quantity is treated explicitly. Rewriting (7) in matrix notation including an error vector ϵ , one obtains

$$\mathbf{g}_{k-1} + \epsilon = \mathbf{A}_{k-1} \mathbf{C}_k \quad (8)$$

where now the subscript k denotes the iterative step. Instead of solving (8) it is convenient to solve the equation

$$\mathbf{g}'_{k-1} + \epsilon = \mathbf{A}_{k-1} \mathbf{C}'_k \quad (9)$$

where

$$\mathbf{g}'_{k-1} = \mathbf{g}_{k-1} - \bar{\mathbf{g}} \quad \text{and} \quad \mathbf{C}'_k = \mathbf{C}_k - \bar{\mathbf{C}}.$$

The barred quantities pertain to some reference condition with which the solution may be smoothed against. It is desired to smooth the solution to the point where the condition

$$\sum_i (I_i - \hat{I}_i)^2 = \sum_i \epsilon_i^2 \approx \sigma^2 \quad (10)$$

is met (thus accounting for the random errors of observation) where \hat{I}_i is the radiance calculated from the solution vector \mathbf{C} .

Since in many instances the tropospheric temperature distribution may be adequately characterized by a single temperature lapse rate, it is convenient to let the reference atmosphere be characterized by

$$\bar{T}(p) = \bar{C}_1 + \bar{C}_2 \ln \frac{p}{p_0}, \quad p_t \leq p \leq p_0. \quad (11)$$

Equation (11) is identical to (6) for the condition $C_2 = C_3$. Equation (7) may be rewritten for the reference state with bars as

$$g_i^{(k-1)} = \sum_{j=1}^3 \bar{C}_j^{(k)} \bar{a}_{ij}^{(k-1)} \quad (12)$$

where

$$\bar{a}_{i1}^{(k-1)} = a_{i1}^{(k-1)} \quad \text{and} \quad \bar{a} = \int_{p_t}^{p_0} \alpha_i^{(k-1)}(p) dp.$$

In this paper the three observations in the 15μ CO_2 band and the observation in the 11μ window are to be used to derive the temperature profile. Since (12) is then overdetermined by two equations, a least squares solution of (12) should be relatively insensitive to random errors

of measurement. The least squares solution to (8), written for the reference state with bars, obtained by minimizing $\epsilon \cdot \epsilon$ with respect to k , \bar{C} is

$$\bar{C}_k = (\bar{A}_{k-1}^T \bar{A}_{k-1})^{-1} \bar{A}_{k-1}^T \bar{g}_{k-1} \quad (13)$$

where A^T is the transpose of A and A^{-1} is the inverse of A .

A solution to (9) may now be obtained by minimizing the sum of the squares of the temperature differences between the solution and reference profiles. The expression to be minimized is

$$\int_{p_t}^{p_0} \left(\sum_{j=1}^3 C_j^{(k)} b_j \right)^2 dp + \frac{1}{\gamma} \sum_i \epsilon_i^2 \quad (14)$$

where

$$b_2 = 1 \quad p_t \leq p \leq p_0$$

$$b_2 = \ln \frac{p_c}{p_0}, \quad b_3 = \ln \frac{p}{p_c} \quad p_t \leq p \leq p_c$$

$$b_2 = \ln \frac{p}{p_0}, \quad b_3 = 0 \quad p_c \leq p \leq p_0$$

and γ is a smoothing parameter whose value depends on the size of $\sum_i \epsilon_i^2$. This yields the general form of the solution given by Twomey [11]

$$C'_k = (A_{k-1}^T A_{k-1} + \gamma H)^{-1} A_{k-1}^T g'_{k-1} \quad (15)$$

where here the elements of the H matrix are given by

$$h_{11} = p_0 - p_t; \quad h_{22} = \int_{p_c}^{p_0} \left(\ln \frac{p}{p_0} \right)^2 dp + (p_c - p_t) \left(\ln \frac{p_c}{p_0} \right)^2;$$

$$h_{33} = \int_{p_t}^{p_c} \left(\ln \frac{p}{p_c} \right)^2 dp;$$

$$h_{12} = h_{21} = \int_{p_c}^{p_0} \ln \frac{p}{p_0} dp + (p_c - p_t) \ln \frac{p_c}{p_0};$$

$$h_{13} = h_{31} = \int_{p_t}^{p_c} \ln \frac{p}{p_c} dp;$$

$$h_{23} = h_{32} = \left(\ln \frac{p_c}{p_0} \right) \int_{p_t}^{p_c} \ln \frac{p}{p_c} dp.$$

It is apparent from (15) that as γ increases in value the solution vector C approaches the bias vector \bar{C} (i.e., $C' \rightarrow 0$). However, since the bias vector used here should give a reasonable approximation to the actual temperature profile the possibility of arriving at a meteorologically acceptable solution, even for relatively large random errors, is retained regardless of how large γ must be.

The solution (15) requires the level, p_c , dividing the two layers of constant lapse rate to be specified. The optimum p_c level is that one which enables a solution for the temperature profile, $T(p)$, to be obtained such that

$$\int_{p_0}^{p_t} [T(p) - \hat{T}(p)]^2 dp = \text{minimum}$$

although the optimum p_c level cannot be specified unless

the actual temperature profile, $T(p)$, is known; it is also physically associated with the condition

$$\sum_{i=1}^4 [I(\Delta\nu_i) - \hat{I}(\Delta\nu_i, p_c)]^2 = \text{minimum}. \quad (16)$$

The radiances calculated from the solution profiles are a function of p_c since (15) is overdetermined. Thus, although the temperature solution is a function of p_c , the optimum solution can be estimated as that solution which satisfies (16).

MOISTURE MODEL

The water vapor distribution can be solved almost simultaneously with the temperature profile by employing the Taylor expansion

$$\tau_{k+1}^*(p) = \tau_k^*(p) + \left[\frac{\partial \tau^*(p)}{\partial \ln U(p)} \right]_k \ln \frac{U_{k+1}(p)}{U_k(p)}. \quad (17)$$

$U(p)$ is the reduced H_2O mass above the level p and is defined by

$$U(p) = \frac{1}{g} \int_0^p w(p) \left(\frac{p}{p_0} \right)^n dp \quad (18)$$

where $w(p)$ is the water vapor mixing ratio and n is the pressure reduction power which is assumed to be 0.72 after Möller and Raschke [6]. The "power law" model for the $w(p)$,

$$w(p) = w(p_0) \left(\frac{p}{p_0} \right)^\lambda \quad 0 \leq p \leq p_0, \quad (19)$$

is assumed, and λ in this paper is assumed to be equal to a climatological value. It then follows from (18) and (19) that

$$w_k(p) = \frac{g U_k(p) (\lambda + n + 1)}{p}$$

and

$$\frac{U_k(p)}{U_{k-1}(p)} = \frac{w_k(p)}{w_{k-1}(p)}. \quad (20)$$

Since the stratosphere is completely transparent in the 18–20 μ spectral region (as shown by fig. 1), the difference between the observed radiance and the radiance calculated from the temperature and moisture profile obtained in the k th iteration may be approximated by

$$I(\Delta\nu_5) - \hat{I}^{(k)}(\Delta\nu_5) = C_2^{(k)} \int_{p_c}^{p_0} \frac{\tau_5^{*(k)}(p)}{p} \left[\frac{\partial B_5(p)}{\partial T(p)} \right]_k dp + C_3^{(k)} \int_{p_t}^{p_c} \frac{\tau_5^{*(k)}(p)}{p} \left[\frac{\partial B_5(p)}{\partial T(p)} \right]_k dp \quad (21)$$

where $\tau^{*(k)}(p)$ is the deviation of the actual transmissivity function from that estimated in the k th iteration. The relation

$$\frac{\partial \tau_5^{*(k)}(p)}{\partial \ln U(p)} = \frac{\partial \tau_5^{*(k)}(p)}{\partial p} \frac{\partial p}{\partial \ln U(p)} = \frac{p}{n + \lambda + 1} \frac{\partial \tau_5^{*(k)}(p)}{\partial p},$$

which is derived from (18) and (19), is used with (17)

and (20) to obtain the following solution for the mixing ratio profile for the $(k+1)$ th iteration as a function of the profiles calculated for the k th iteration:

$$w_{k+1}(p) = w_k(p) \exp \left[\frac{(g_5 - g_5^{(k)})(n + \lambda + 1)}{C_2^{(k)} \beta^{(k)}(p_c, p_0) + C_8^{(k)} \beta^{(k)}(p_t, p_c)} \right] \quad (22)$$

where

$$\beta(p_1, p_2) = \int_{p_1}^{p_2} \left[\frac{\partial B_5(p)}{\partial T(p)} \right]_k \frac{\partial \tau_5^{*(k)}(p)}{\partial p} dp$$

and

$$g_5 - g_5^{(k)} = I(\Delta\nu_5) - \hat{I}^{(k)}(\Delta\nu_5).$$

The solution for the moisture distribution of the reference atmosphere in which $\bar{C}_3 = \bar{C}_2$ is obviously

$$\bar{w}_{k+1}(p) = \bar{w}_k(p) \exp \left[\frac{(g_5 - \bar{g}_5^{(k)})(n + \lambda + 1)}{\bar{C}_2^{(k)} \beta^{(k)}(p_t, p_0)} \right]. \quad (23)$$

It is noted that the solution given by (22) is restricted to the power law form, (19). Although this form prohibits the derivation of any detailed water vapor structure, it is adequate to account for the water vapor dependence of the transmissivity functions used to derive the temperature profile as well as provide an accurate estimate of the total tropospheric precipitable water content. A more detailed structure may, in theory, be derivable from additional measurements in other regions of the water vapor absorption spectrum.

NUMERICAL METHOD

As in any iterative procedure, an initial estimate of the parameters to be calculated must be made. In this case physically reasonable initial estimates can readily be made. For instance, the surface temperature may be assumed to be equal to the equivalent blackbody temperature measured in the atmospheric window region. A good initial estimate of the tropospheric lapse rate and total precipitable water, which specifies the mixing ratio profile (equations (20) and (19)), may be made from climatological averages. Representative values for the moisture parameter λ have been tabulated by the author (Smith [8]). As will be shown, however, the final solution obtained by the method outlined here is not highly dependent on the initial conditions so that only a very crude initial estimate of the temperature and moisture profiles is necessary.

The procedure for calculating the temperature and moisture profile of the troposphere from the radiative measurements cited in this paper may now be summarized as follows:

1) From an initial estimate of the temperature and moisture distribution and the observed radiances, the vector \mathbf{g} and matrix $\bar{\mathbf{A}}$ are calculated.

2) Utilizing the least squares solution given by (13) the vector $\bar{\mathbf{C}}$ is calculated from the g_i and \bar{a}_{ij} pertaining to the 15μ and 11μ spectral regions. The corresponding ref-

erence temperature profile is then calculated from equation (11).

3) $\bar{\mathbf{C}}_k$ and \bar{a}_{5j} which pertain to the 18.7μ spectral region are used. Then, $g_5^{(k)}$ is calculated from equation (12) and utilized in (23) to provide the next estimate of the water vapor mixing ratio profile and subsequently a better approximation of the transmittances $\tau_i^*(p)$.

4) Steps 1-4 are repeated until the condition

$$\frac{1}{p_0 - p_t} \int_{p_t}^{p_0} |T_k(p) - T_{k-1}(p)| dp \leq 0.25^\circ$$

is satisfied.

5) The reference profiles obtained above are then used as initial estimates in a second iterative loop and to define $\bar{\mathbf{g}}$ as given by (12). The matrix $\bar{\mathbf{A}}$ is redefined by (7). The procedure used in this loop is analogous to that given above except that the temperature solution is obtained from equations (15), (5), and (6) for a finite number of p_c values ranging between p_t and p_0 . The final solution in each step is taken as that which satisfies equation (16). The moisture solution is then calculated from (22) and the procedure iterated until the condition given in step 4) is once again met. The calculations in this loop are made for that γ value which smooths the solution to the point where (10) is closely approximated.

5. RESULTS

On May 8, 1966, a NASA balloon-borne interferometer measured several spectra of infrared radiance between 500 cm^{-1} and 2000 cm^{-1} (i.e., 20μ - 5μ). The spectral resolution of the measurements which were taken from the 7-mb. level (110,000 ft.) over Palestine, Texas, is about 5 cm^{-1} . The data obtained between 0730 CST and 1411 CST have been listed elsewhere by Chaney, Loh, and Surh [2].

The infrared radiances obtained in a spectral scan may be used to approximate the infrared radiances which would have been measured by the modified MRIR. The radiances, which were approximated for each spectral interval by

$$I(\Delta\nu_i) = \int_{\Delta\nu_i} \phi_i(\nu) I(\nu) d\nu / \int_{\Delta\nu_i} \phi_i(\nu) d\nu, \quad i=1, 2, 3, 4, 5$$

where $\phi_i(\nu)$ was assumed to be given by (3), are summarized in figure 2. As can be seen, the diurnal variations of the radiance in each spectral interval were mainly due to variations in surface temperature and/or cloud amount as clearly portrayed by the radiance measured in the atmospheric window region (825 - 975 cm^{-1}). Exceptions to this general trend are noted for: 1) the 500 - 570-cm^{-1} interval between 0810 and 1009 CST as well as between 1134 and 1411 CST, 2) the 717.5 - 757.5-cm^{-1} interval between 0730 and 0810 CST, and 3) all the carbon dioxide spectral intervals between 0906 and 1009 CST. Although the deviations from this trend for the 500 - 570-cm^{-1} interval could result from significant variations in water vapor

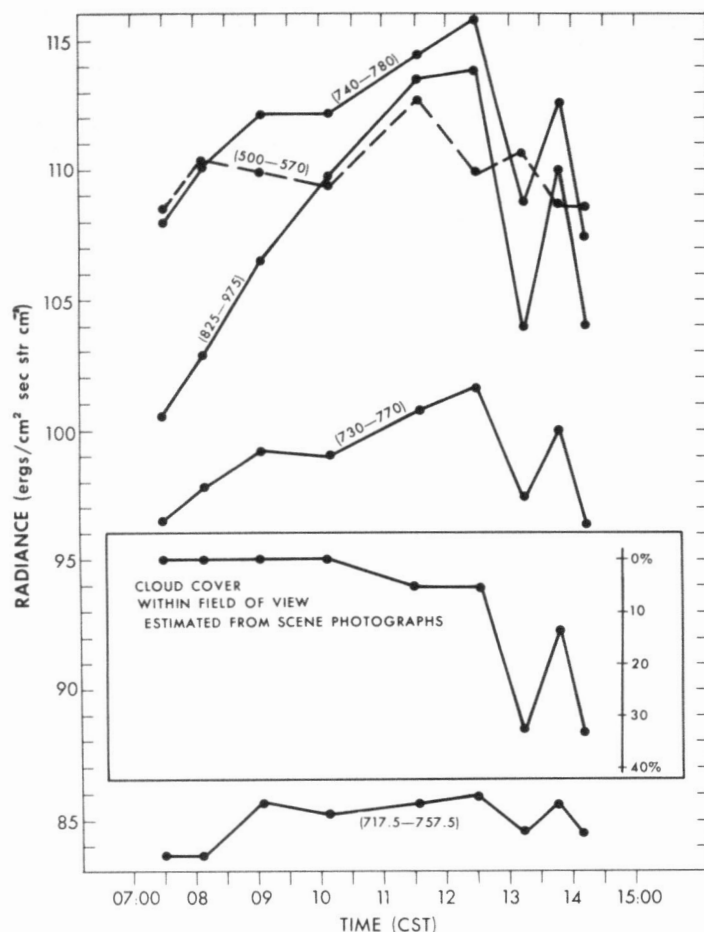


FIGURE 2.—Diurnal variation of the radiances measured by the interferometer and (inset) the cloud cover within the field of view of the interferometer for Palestine, Texas.

TABLE 1.—Radiances ($\text{ergs}/(\text{cm}^2 \text{ sec. strdn. cm}^{-1})$) obtained from the first four interferometer scans taken at 0730 CST.

Scan	825-975 cm^{-1}	740-780 cm^{-1}	730-770 cm^{-1}	717.5-757.5 cm^{-1}	500-570 cm^{-1}
1	100.60	110.25	99.73	84.51	109.69
2	99.53	108.75	97.93	84.84	112.51
3	102.20	106.81	93.55	81.07	103.01
4	100.44	108.01	98.09	84.71	109.70

and/or atmospheric temperature, they are probably due to the relatively high uncertainties of measurement which are caused by the drop of instrument sensitivity in this spectral region (Chaney et al. [2]). Likewise, the decrease in the radiances observed in the CO_2 spectral intervals during periods of increasing ground temperature may be attributed to instrumental errors which have been shown by Chaney et al. to be higher in these regions than in other portions of the $15\mu \text{CO}_2$ band. The influence of these errors on the derived temperature and moisture profiles is illustrated below.

Before a solution for the temperature profile may be obtained, it is necessary to estimate the *random* error of the radiance observations so as to choose the appropriate value of the smoothing parameter, γ . The radiances obtained from the first four interferometer scans (table 1) were chosen for this purpose. As may be seen from table 1, scans 1, 2, and 4 are fairly consistent; whereas scan 3 is totally inconsistent. Since all four scans were measured

over a 60-sec. period, the discrepancies noted may be attributed to instrumental noise. Due to the large systematic error in the radiances measured in scan 3 (i.e., all the radiances with exception of that measured in the 825-975- cm^{-1} interval are significantly lower than those measured in scans 1, 2, and 4), this scan was deleted in estimating the random error. The average deviation of the radiances measured in scans 1, 2, and 4 from their respective averages is $0.65 \text{ erg}/(\text{cm}^2 \text{ sec. strdn. cm}^{-1})$, this implies a random error in the scan 3 average values of about $0.4 \text{ erg}/(\text{cm}^2 \text{ sec. strdn. cm}^{-1})$.

Figure 3a shows the temperature and water vapor mixing ratio profiles calculated from the 3-scan (1, 2, and 4) average values. The solutions were obtained for a γ value of 10^{-7} which resulted in an average difference between the observed radiances and those computed from the calculated profiles equal to the random error estimated above. The dots and triangles are neighboring radiosonde observations; whereas the solid curves are the calculated profiles. The dashed lines represent the initial profiles estimated from the assumptions that: 1) the surface temperature was equal to the equivalent blackbody temperature measured in the window spectral interval, 2) the troposphere was isothermal, and 3) the total precipitable water was 6 cm. The moisture parameter λ was assumed to be 2.6 which is the Northern Hemispheric average value given by Smith [8]. These very crude initial estimates were chosen to demonstrate the independence of the final solution on the initial conditions. As may be seen, the agreement between the final solutions and the radiosonde observations is good. Furthermore, only five iterations were required to obtain these solutions.

Figures 3b, 3c, and 3d display the solutions calculated from the averages of four successive scans measured around the local times shown. The effects of the instrumental errors previously noted at 0810 CST and 1009 CST are clearly portrayed in these solutions. The relatively small bias errors in the 0810 temperature profile (fig. 3b) are due in part to the small negative error in the 717.5-757.5- cm^{-1} radiance and an apparent positive error in the 500-570- cm^{-1} radiance. The positive error in the latter spectral region is suggested by the fact that the water vapor solutions obtained at 0730 CST and 0930 CST are in good agreement and the radiance measured at 0810 CST is significantly higher than those measured at 0730 CST and 0930 CST in this water vapor spectral interval. The temperature solution (not shown) obtained by utilizing the radiosonde mixing ratios was slightly improved below the 600-mb. level. The temperature errors above this level are probably due to the negative error in the 717.5-757.5- cm^{-1} radiance. For the 1009 CST solution (fig. 3d) the opposite was true. The large errors in the temperature profile contributed substantially to the errors in the mixing ratio profile. Whereas no substantial change occurred in the 1009 CST temperature solution by employing the radiosonde mixing ratio profile, a large change occurred in the calculated mixing ratio profile by utilizing the radiosonde temperature profile. These results indicate, as expected, that the water vapor calculation is much more

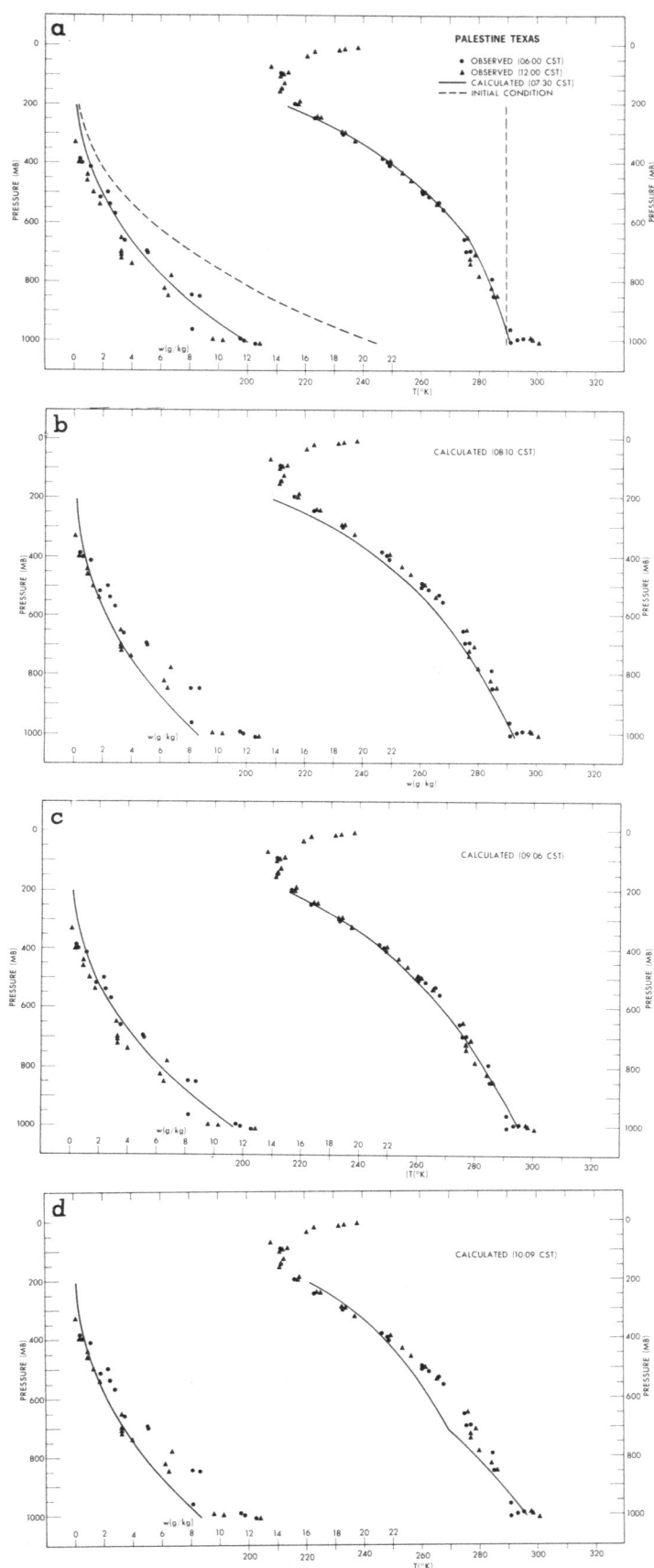


FIGURE 3.—Solutions for the temperature and moisture profiles at Palestine, Texas. The dots and triangles are radiosonde values observed at 0600 cst and 1200 cst, respectively, and the solid curves are the calculated profiles. (a) Calculations from the 3-scan (1, 2, and 4) average values. (b)–(d) Calculations from averages of form successive scans measured around (b) 0810 cst, (c) 0906 cst, and (d) 1009 cst.

TABLE 2.—Summary of infrared radiances ($\text{ergs}/(\text{cm}^2 \text{ sec. strdn. cm.}^{-1})$), total precipitable water Q (cm.) and required number of iterations

(a) 0730 cst	Observed	Calculated	Difference
I_1	100.2	100.5	−0.3
I_2	109.0	108.5	+0.5
I_3	98.6	98.5	+0.1
I_4	84.7	85.1	−0.4
I_5	110.5	109.9	+0.6
Q	3.45	3.40	−.05
Number of Iterations: 5			
(b) 0810 cst	Observed	Calculated	Difference
I_1	102.9	103.0	−0.1
I_2	110.1	109.6	+0.5
I_3	97.8	98.3	−0.5
I_4	83.5	83.6	+0.1
I_5	110.4	109.8	+0.6
Q	3.45	2.51	−.94
Number of Iterations: 8			
(c) 0906 cst	Observed	Calculated	Difference
I_1	106.6	106.6	0.0
I_2	112.2	111.6	+0.6
I_3	99.2	100.2	−1.0
I_4	85.7	85.3	+0.4
I_5	109.9	109.4	+0.5
Q	3.45	3.25	−0.20
Number of Iterations: 8			
(d) 1009 cst	Observed	Calculated	Difference
I_1	109.8	109.2	+0.6
I_2	112.1	112.5	−0.4
I_3	99.0	100.0	−1.0
I_4	85.3	84.3	+1.0
I_5	109.3	109.4	−0.1
Q	3.45	2.53	−0.92
Number of Iterations: 13			

sensitive to errors in the radiances used to calculate the temperature profile than the temperature calculation is to errors existing in the radiance used to calculate the water vapor profile. It is reemphasized that the large errors occurring in the 1009 cst solution resulted from the large negative errors (estimated to be greater than $2 \text{ ergs}/(\text{cm}^2 \text{ sec. strdn. cm.}^{-1})$) apparently inherent in the entire $717.5\text{--}780\text{-cm.}^{-1}$ interval. Since the errors in both the 0810 cst and 1009 cst solutions are in the same direction, one might question the transmittances used in the calculations. However, the good agreement obtained in the 0730 cst and 0906 cst solutions rule out this argument.

Table 2 summarizes the observed radiances and the number of iterations utilized to obtain each solution shown in figure 3, the radiances calculated from these solutions, as well as the observed and calculated total precipitable water. It is evident from comparing table 2 with figure 3 that the accuracy of the solutions is related to the number of iterations required to obtain these solutions as well as the average deviation between the observed and calculated radiances. Hence, untolerable solutions, such as those obtained for 1009 cst, may be recognized objectively from these quantities. It is also noted that the accuracy of the total precipitable water estimates is highly dependent upon the accuracy of the temperature profile calculations.

6. DATA ANALYSIS IN THE PRESENCE OF CLOUDS

The major obstacle to be overcome, before satellite infrared radiation observations may be utilized to obtain atmospheric temperature and moisture profiles on a global

scale, is that of adequately reducing such data over the vast cloudy regions of the earth. Clouds attenuate the infrared radiation emitted from the earth's surface and atmosphere below. If the attenuation by clouds is unaccounted for, the solutions obtained for the temperature and moisture profiles of the cloudy regions will contain intolerable errors.

The problem of inferring accurate tropospheric temperature and moisture profiles *directly* from cloud attenuated radiances is difficult. The reason is that such a solution must account for the heights, the amounts, and the opacities of the various clouds which might exist within the field of view of the sensing instrument. Since a number of radiance measurements must be given up to solve for these parameters, the number of independent radiance observations that may be used to solve for the profiles is reduced. The fact that the opacities of many clouds (e.g., cirroforms) are highly dependent upon spectral frequency further complicates the problem.

It is apparent that it is convenient to utilize only "clear column" radiances to derive tropospheric temperature and moisture profiles. This suggests that such radiances be obtained by a radiometer capable of resolving very small areas on the earth's surface, hence having the capability of "seeing" through any holes which may exist in regions of relatively dense cloud cover. However, a radiometer of finite resolution may often view columns that are partially cloudy and an objective means of differentiating between radiances measured over partially cloudy and clear columns is difficult. For this reason an objective method has been developed for calculating clear column radiances from radiances which are measured over partly cloudy regions.

Consider a field of radiation measurements provided by a satellite-borne radiometer scanning in a direction perpendicular to the orbital path. Assume the angular resolution is sufficiently high so that each resolution element encloses an area much smaller than that area for which it is desired to calculate the average temperature and moisture profiles. As previously shown by the author (Smith [9]) the radiance measured over each resolution element is given for any frequency interval, $\Delta\nu_i$ by

$$I(\Delta\nu_i) = NI_{CD}(\Delta\nu_i) + (1-N)I_{CR}(\Delta\nu_i) \quad (24)$$

where N is the amount of cloud cover within each resolution element, $I_{CD}(\Delta\nu_i)$ is the average radiance arising from the cloudy portion and $I_{CR}(\Delta\nu_i)$ is the radiance arising from the clear portion of each resolution element. Writing (24) for two different resolution elements subscripted 1 and 2 gives

$$I_1(\Delta\nu_i) = N_1 I_{CD1}(\Delta\nu_i) + (1-N_1) I_{CR1}(\Delta\nu_i) \quad (25)$$

$$I_2(\Delta\nu_i) = N_2 I_{CD2}(\Delta\nu_i) + (1-N_2) I_{CR2}(\Delta\nu_i). \quad (26)$$

A solution for the average "clear column" radiance may be obtained if

$$N_1 \neq N_2.$$

The fulfillment of this requirement can easily be determined from the measured window radiances, $I(W)$, since for this condition

$$I_1(W) \neq I_2(W).$$

If the resolution elements are relatively small and adjacent then it is reasonable to assume that

$$I_{CD2}(\Delta\nu_i) = I_{CD1}(\Delta\nu_i)$$

and

$$I_{CR}(\Delta\nu_i) = I_{CR1}(\Delta\nu_i) = I_{CR2}(\Delta\nu_i)$$

where $I_{CR}(\Delta\nu_i)$ is the clear column radiance which is assumed to be constant throughout both resolution elements. Under these assumptions the following solution may be obtained for $I_{CR}(\Delta\nu_i)$ from equations (25) and (26):

$$I_{CR}(\Delta\nu_i) = \frac{I_2(\Delta\nu_i) - N^* I_1(\Delta\nu_i)}{1 - N^*} \quad (27)$$

where $N^* = N_1/N_2$. It is evident that if N^* is known the clear column radiance for any frequency interval may be calculated from measurements over two adjacent cloudy columns. N^* may be calculated from simultaneous measurements of the radiance in the window region. Rearranging (27) yields

$$N^* = \frac{I_1(W) - I_{CR}(W)}{I_2(W) - I_{CR}(W)}. \quad (28)$$

$I_{CR}(W)$ may be either approximated from an *in situ* observation of surface temperature or measured directly by a very high angular resolution window radiometer. Since a radiometer capable of measuring the infrared radiance in the 10–11 μ window region arising from an area of the earth which is less than 0.5 \times 0.5 n.mi.² is presently scheduled to be flown on the Applications A Apollo Satellite, the latter approach may be taken for the Apollo modified MRIR experiment. In any event the quantity $I_{CR}(W)$ appears in both the numerator and the denominator of (28) so that the accuracy required is generally less than that of $I_1(W)$ and $I_2(W)$. Since N^* is frequency independent, being the ratio of the cloud amounts existing within the two resolution elements, the value obtained in (28) may be used in (27) to calculate the radiances arising from the clear columns in other spectral regions.

The major assumption made in the above development is that the average radiance arising from the cloud covered columns is the same for both resolution elements. This implies that, if the clouds are black, the heights of the clouds are the same. To insure that the heights of the clouds do not differ radically among adjacent resolution elements, the field of view of the sensing system should be as small as practically possible.

It is also apparent from (27) that the error of $I_c(\Delta\nu_i)$ tends to inflate by $1/(1-N^*)$ the error of the observations. Therefore, if the field of view of the sensing instrument is small, weighted average clear column radiances can be calculated over geographical areas larger than

TABLE 3.—Summary of radiances measured over cloudy columns at Palestine, Texas

Time (cst)	Measured Radiances				
	825-975 cm. ⁻¹	740-780 cm. ⁻¹	730-770 cm. ⁻¹	717.5-757.5 cm. ⁻¹	500-570 cm. ⁻¹
1312.....	103.9	108.7	97.4	84.6	110.6
1348.....	110.1	112.7	100.0	85.7	108.6
1411.....	103.9	107.3	96.4	84.5	108.5
	Calculated Clear Column Radiances				
1312-1348.....	*113.94	115.2	101.6	86.3	107.3
1348-1411.....	*113.94	116.1	102.4	86.5	108.6
Average.....	*113.94	115.7	102.0	86.4	108.0

*Assumed to be equal to the radiance measured at 1231 cst.

that resolved in an individual observation by

$$\bar{I}_c(\Delta\nu_i) = \frac{\sum_{j=1}^n W_j I_{cj}(\Delta\nu_i)}{\sum_{j=1}^n W_j}$$

where W_j , the weight, is $(1 - N^*)$. As indicated earlier, the radiometer planned to be flown on the Apollo will obtain a 10×10 matrix of spatially independent observations, for each spectral interval, over a 100 n.mi.² area. Since a total of 342 different combinations of adjacent elements can be formed from the 10×10 matrix, than if N^* differs from zero or unity for each combination, it is evident that there are 342 independent estimates of $I_c(\Delta\nu_i)$ to determine the $\bar{I}_c(\Delta\nu_i)$'s and consequently the average temperature and moisture profiles for the area. Thus, the effect of random observational errors and differing cloud heights tends to be reduced to an insignificant level.

A distinction between this method and that previously proposed by the author (Smith [9]) is in order. In the previously proposed method the equation for $I_{CR}(\nu)$ and N^* were similar but $I_1(\nu)$ was defined as the average of all the radiances in the total area of observation and $I_2(\nu)$ was defined as the average of all the radiances less than the total average. It is implicit in the former equations that the cloud column radiances are constant throughout the entire region of observation in contrast to the requirement that the cloud column radiances be constant among two adjacent resolution elements. Since the latter assumption is more physically reasonable, better results will be obtained by the method outlined here.

The radiances measured at 1312, 1348, and 1411 CST by the balloon-borne interferometer simulate radiance observations of three adjacent resolution elements which would have been observed by a radiometer scanning the atmosphere over Palestine, Texas. These radiances have been used to calculate the clear column radiances by the method outlined above. Table 3 gives a summary of both the observed cloudy column radiances as well as the calculated clear column radiances. Since the observed window radiances for 1312 and 1411 CST are equivalent only two independent calculations could be made. The

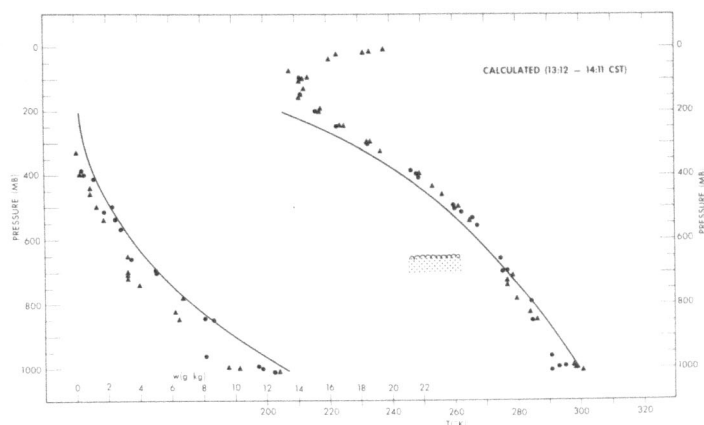


FIGURE 4.—Temperature and moisture calculated from the cloud attenuated radiances observed at Palestine, Texas. The dots and triangles are radiosonde values observed at 0600 CST and 1200 CST, respectively, and the solid curves are the profiles calculated from the radiances observed between 1312 CST and 1411 CST.

clear column window radiance, $I_{CR}(W)$, was assumed to be given by the window radiance observed over the nearly clear atmosphere at 1231 CST (see fig. 2). The calculated N^* value was 0.386 which compares favorably with that estimated from the scene photographs (see fig. 2) of 0.363. Considerable differences are noted in the two independent calculations resulting from the differences which existed in the observed radiances at 1312 and 1411 CST. These differences are probably due to errors of observations.

The average values of the calculated clear column radiances were then utilized to calculate the temperature and moisture profiles at Palestine, Texas. The results of this calculation are shown in figure 4. Considering the possible observational errors and the fact that only two independent estimates of the clear column radiances were used in this calculation, the method of calculation is felt to be successful. The fact that the errors in the temperature profile are in the same sense as those arising in the soundings obtained earlier from observed clear column radiances further implies that the errors are not due to the method of calculating the clear column radiances.

7. CONCLUSION

Considering the probable errors of measurement as well as the probable errors inherent in the transmissivity calculations, the results obtained in this study indeed affirm the possibility of deriving accurate estimates of tropospheric structure from satellite radiometer measurements. (See discussions by several authors [1, 3, 4, 5, 12, 13, 14, 15].) It is felt that a significant advancement has been made toward defining an objective and efficient method for obtaining such estimates on a global scale from filtered radiometer measurements. A program is currently being implemented to provide these measurements which are so urgently needed for more precise weather analysis and forecasting.

ACKNOWLEDGMENTS

The research reported in this paper could not have been conducted without the former endeavors of many others. These researchers and their works, as given in the references, are fully acknowledged. The author is also indebted to Mr. H. E. Fleming of the National Environmental Satellite Center for his fruitful suggestions on various mathematical aspects of this problem.

REFERENCES

1. L. W. Chaney, S. R. Drayson, and C. Young, "Fourier Transform Spectrometer-Radiative Measurements and Temperature Inversion," *Applied Optics*, vol. 6, No. 2, Feb. 1967, pp. 347-349.
2. L. W. Chaney, L. T. Loh, and M. T. Surh, "A Fourier Transform Spectrometer for the Measurement of Atmospheric Thermal Radiation," *Technical Report*, Contract NASr-54(03), College of Engineering, The University of Michigan, Ann Arbor, May 1967, 113 pp.
3. B. J. Conrath, "Inverse Problems in Radiative Transfer: A Review," *NASA Report X-622-67-57*, Goddard Space Flight Center, Feb. 1967, 35 pp.
4. L. D. Kaplan, "Inference of Atmospheric Structure From Remote Radiation Measurements," *Journal of the Optical Society of America*, vol. 49, No. 10, Oct. 1959, pp. 1004-1007.
5. J. I. F. King, "Inversion by Slabs of Varying Thickness," *Journal of the Atmospheric Sciences*, vol. 21, No. 3, May 1964, pp. 324-326.
6. F. Möller and E. Raschke, "Evaluation of TIROS III Radiation Data," *NASA Contractor Report CR-112*, NASA Research Grant NsG-305, University of Munich, Germany, for National Aeronautics and Space Administration, Washington, D.C., Nov. 1964, 84 pp.
7. D. L. Phillips, "A Technique for the Numerical Solution of Certain Integral Equations of the First Kind," *Journal of the Association for Computing Machinery*, vol. 9, No. 1, Jan. 1962, pp. 84-97.
8. W. L. Smith, "Note on the Relationship Between Total Precipitable Water and Surface Dew Point," *Journal of Applied Meteorology*, vol. 5, No. 5, Oct. 1966, pp. 726-727.
9. W. L. Smith, "An Iterative Method for Deducing Tropospheric Temperature and Moisture Profiles From Satellite Radiation Measurements," *Monthly Weather Review*, vol. 95, No. 6, June 1967, pp. 363-369.
10. V. R. Stull, P. J. Wyatt, and G. N. Plass, "The Infrared Absorption of Carbon Dioxide," *Infrared Transmission Studies Final Report*, vol. III, Contract AF 19(604)-7479, Aeronutronic Division, Ford Motor Company, Jan. 1963, 36 pp.
11. S. Twomey, "On the Numerical Solution of Fredholm Integral Equations of the First Kind by Inversion of the Linear System Produced by Quadrature," *Journal of the Association for Computing Machinery*, vol. 10, No. 1, Jan. 1963, pp. 97-101.
12. D. Q. Wark, "On Indirect Temperature Soundings of the Stratosphere From Satellites," *Journal of Geophysical Research*, vol. 66, No. 1, Jan. 1961, pp. 77-82.
13. D. Q. Wark and H. E. Fleming, "Indirect Measurements of Atmospheric Temperature Profiles From Satellites: I. Introduction," *Monthly Weather Review*, vol. 94, No. 6, June 1966, pp. 351-362.
14. D. Q. Wark, F. Saiedy, and D. G. James, "Indirect Measurements of Atmospheric Temperature Profiles From Satellites: VI. High-Altitude Balloon Testing," *Monthly Weather Review*, vol. 95, No. 7, July 1967, pp. 468-479.
15. G. Yamamoto, "Numerical Method for Estimating the Stratospheric Temperature Distribution From Satellite Measurements in the CO₂ Band," *Journal of Meteorology*, vol. 18, No. 5, Oct. 1961, pp. 581-588.

[Received November 6, 1967; revised March 19, 1968]